Electrostatic Association of Ammonium Functionalized Layered Transition Metal Dichalcogenides with an Anionic Porphyrin

Ruben Canton-Vitoria, Christina Stangel and Nikos Tagmatarchis[*]

Theoretical and Physical Chemistry Institute, National Hellenic Research Foundation, 48 Vassileos Constantinou Avenue, 11635 Athens, Greece.

ABSTRACT: Functionalization of exfoliated MoS_2 and WS_2 with 1,2-dithiolane *tert*-butyl carbamate (BOC), followed by acidic deprotection of the BOC moiety, resulted in the preparation of ammonium modified layered transition metal dichalcogenides **3a** and **3b**. The functionalized materials were sufficiently characterized by complementary spectroscopic, thermal and microscopy means, while the amount of ammonium units on the modified MoS_2 and WS_2 was calculated with the aid of Kaiser test. The positive charges, owed to the presence of ammonium units, on MoS_2 and WS_2, were exploited to bring in contact via electrostatic attractive forces an anionic porphyrin bearing a carboxylate unit, yielding porphyrin/MoS_2 and porphyrin/WS_2 ensembles **5a** and **5b**, respectively. Titration assays disclosed efficient photoluminescence quenching of the porphyrin by MoS_2 and WS_2 within the nanoensembles **5a** and **5b**, while in combination with time-resolved photoluminescence measurements, revealed transduction of energy from the photoexcited porphyrin, acting as electron donor, to MoS_2 or WS_2 acting as acceptors.

Two-dimensional nanomaterials, in particular, layered transition-metal dichalcogenides (LTMDs), triggered increasing scientific interest and stay at the forefront of recent research investigations.[1-4] This is not only due to their unique structure in which a metal cation is bonded to four chalcogenide anions in a honeycomb lattice, but also to their exciting physicochemical properties,[5-6] and great potentiality in nanoelectronics, energy storage, sensing, and catalysis.[7-10] Molybdenum and tungsten disulfide, MoS_2 and WS_2, as typical examples of LTMDs, can form different polytypes, semiconducting or metallic, depending on the exfoliation process followed.[11-17] In addition, covalent functionaliza-tion of LTMDs although not fully developed,[18] aids enhancing solubility while keeping apart the exfoliated layers, thus, allowing easier manipulation, processing and properties investigation in wet media. As leading examples, functionalization reactions of MoS_2 with organoiodides or diazonium salts furnishing MoS_2-based materials carrying organic addends at the basal plane,[19-20] and with 1,2-dithiolanes exploiting the high binding affinity for Mo atoms with sulfur vacant sites,[21] should be mentioned. In fact, the latter approach resulted in the introduction of pyrene moieties onto MoS_2 via robust and stable bond formation, despite the lack of detailed analysis for the properties of the hybrid material.[21]
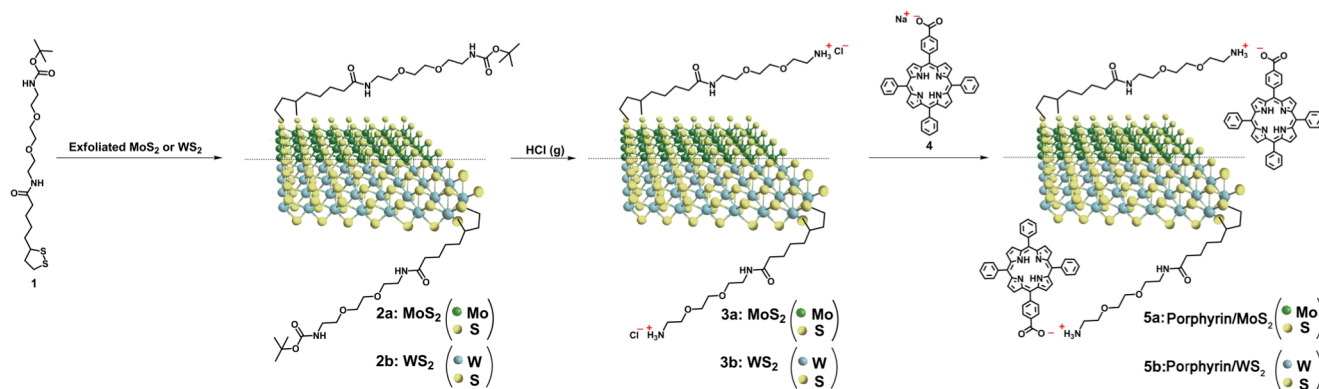
1

Figure 1. Illustrative scheme for the modification of exfoliated MoS$_2$ and WS$_2$ upon reaction with 1,2-dithiolane *tert*-butyl carbamate, furnishing **2a** and **2b**, followed by acidic deprotection to incorporate positively charged ammonium units, yielding **3a** and **3b**, respectively, and the formation of porphyrin/MoS$_2$ **5a** and porphyrin/WS$_2$ **5b** ensembles, via electrostatic attractive interactions between the positively charged ammonium modified MoS$_2$ and WS$_2$ in **3a** and **3b**, respectively, with the negatively charged porphyrin **4**.

Nevertheless, the incorporation of functional species, e.g. photo-active, by other means beyond covalently associated, en route the development of advanced LTMD-based hybrid materials has yet to be realized and surely deserves investigation.

Porphyrins, widely tested in artificial photosynthetic systems, possess an 18π-electron aromatic structure, absorb efficiently light in the visible region with high molar absorbance coefficients, are photochemically stable and have redox potentials and photophysical properties that can be easily tuned by altering the metal center of the macrocycle or through modification of the peripheral substituents.[22, 23] All these features, make porphyrins quite attractive materials for participating in charge-transfer processing as electron donors. Without surprise, a plethora of supramolecularly and covalently associated porphyrins with graphene, the direct all-carbon two-dimensional analogue of LTMDs, have been reported.[24-26]

Considering the ease and reversibility of electrostatic interactions, as means to non-covalently associate species with opposite charges, the aim of the current study is two-fold, namely, to (i) form porphyrin/MoS$_2$ and porphyrin/WS$_2$ ensembles via attractive Coulombic interactions and (ii) investigate intra-ensemble electronic communication between the two species. Herein, modified MoS$_2$ and WS$_2$ bearing ammonium units were electrostatically coupled with an anionic porphyrin possessing a carboxylate group to develop novel donor-acceptor ensembles. Furthermore, intra-ensemble interactions were probed by electronic absorption spectroscopy and steady-state and time-resolved photoluminescence titration measurements to identify photoinduced charge-transfer processes.

Initially, bulk MoS$_2$ and WS$_2$ were exfoliated to semiconducting nanosheets upon treatment with chlorosulfonic acid, according to our previously reported protocol.[12] Next, functionalization of exfoliated MoS$_2$ and WS$_2$ with 1,2-dithiolane *tert*-butyl carbamate (BOC) derivative **1** yielded materials **2a** and **2b**, respectively (Figure 1). The BOC protecting group in **2a** and **2b** can be efficiently removed by acidic treatment with gaseous HCl, to furnish **3a** and **3b**, respectively, in which positively charged ammonium terminating units decorate the edges of modified LTMDs. The work up procedure followed, namely, filtration of the reaction mixture through a PTFE membrane with 0.2 μm pore size followed by extensive washing of the solid residue obtained on top of the membrane filter with dichloromethane, assured that all LTMD-based functionalized materials were free from non-covalently interacting organic species. Zeta-potential measure-
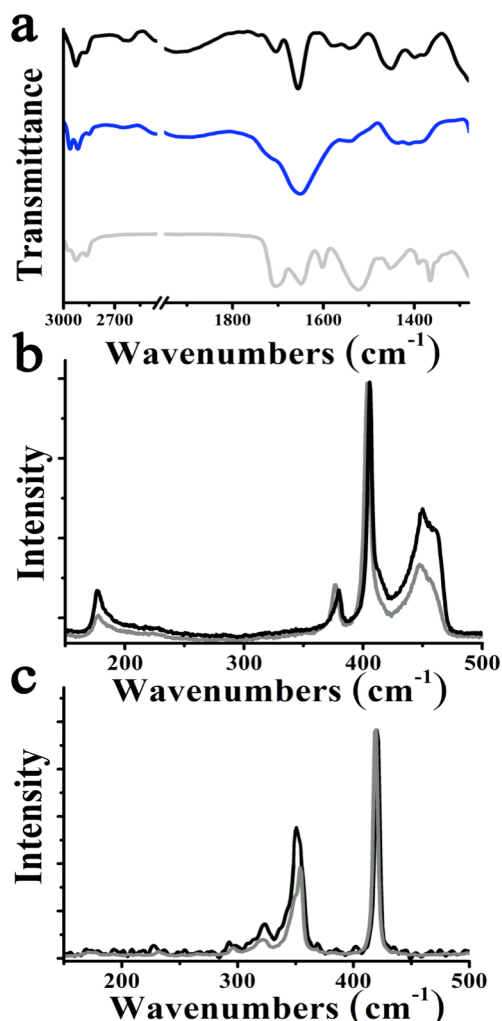

Figure 2. (a) ATR-IR spectra for BOC modified MoS$_2$-based material **2a** (black), ammonium modified MoS$_2$-based material **3a** (blue) and 1,2-dithiolane-BOC derivative **1** (grey), (b) Raman spectra for exfoliated MoS$_2$ (gray) and BOC modified MoS$_2$-based material **2a** (black), normalized at the A$_{1g}$ mode and acquired upon 633 nm excitation. (c) Raman spectra for exfoliated WS$_2$ (gray) and BOC modified WS$_2$-based material **2b** (black), normalized at the A$_{1g}$ mode and acquired upon 514 nm excitation.

ments revealed high difference in the values obtained between exfoliated MoS$_2$ (-28 mV) and WS$_2$ (-24 mV) as compared with those owed to ammonium modified materials **3a** (+2.6 mV) and **3b** (+0.5 mV), respectively. Hence, noting that zeta-potential measures the overall surface charge of the system and not that due to individual species, it is unambiguously proved the presence of positive charges in the ammonium modified LTMDs **3a** and **3b**. Additionally, the amount of ammonium units existing onto modified MoS$_2$ and WS$_2$ was calculated by performing the Kaiser test and found to be 49 and 47 μmol/g for **3a** and **3b**, respectively. Then, having in hand functionalized MoS$_2$ and WS$_2$ carrying positive charges in the form of ammonium units in **3a** and **3b**, respectively, Coulombic interactions were employed to bring them in contact with negatively charged porphyrin **4** bearing a carboxylate moiety, thereby, forming **5a** and **5b** nanoensembles, according to Figure 1.

Spectroscopic evidence for the successful functionalization of exfoliated MoS$_2$ and WS$_2$ with 1,2-dithiolane derivative **1** and the cleavage of the BOC protecting units was delivered by ATR-IR and Raman assays. In particular, the presence of the carbonyl amide and BOC protecting units in **1** gave rise to stretching vibrations identified at 1650 and 1710 cm^{-1}, respectively. The same functional units can be found in **2a**, however, after BOC deprotection only the amide carbonyl is identified at 1650 cm^{-1} in ammonium modified material **3a** (Figure 2a). In addition, characteristic stretching vibrations due to aliphatic C-H units were present in both **2a** and **3a** materials at around 2900-2980 cm^{-1}. Analogously, BOC-protected and ammonium modified WS$_2$-based materials **2b** and **3b** gave rise to similar IR bands (Supporting Information, Figure S1).

Next, Raman spectroscopy upon on-resonance excitation conditions, 633 nm for MoS$_2$ and 514 nm for WS$_2$, revealed richer spectra as compared to those acquired under off-resonance scattering conditions, due to strong electron-phonon coupling interactions.[27] For exfoliated MoS$_2$, four characteristic bands were evident, namely the A$_{1g}$(M)-LA(M) at 185 cm^{-1}, the in-plane E$^1_{2g}$ at 376 cm^{-1}, the out-of-plane A$_{1g}$ at 404 cm^{-1} and the 2LA(M) at 448 cm^{-1} vibration modes. Those bands were found stiffened (blue-shifted) in modified MoS$_2$-based material **2a**, by 2, 4, 1 and 2 cm^{-1}, respectively, namely the A$_{1g}$(M)-LA(M) at 187 cm^{-1}, the E$^1_{2g}$ at 380 cm^{-1}, the A$_{1g}$ at 405 cm^{-1} and the 2LA(M) at 450 cm^{-1} (Figure 2b). In addition, the intensity ratio of 2LA(M) over A$_{1g}$ bands was found 0.52 for **2a**, almost double as compared to the value of 0.27 measured for exfoliated MoS$_2$. Since the 2LA(M) is associated with disorder and defects on MoS$_2$, also providing valuable information on the electronic states of MoS$_2$, the corresponding intensity changes may well be attributed to the incorporation of the organic addends in **2a**, which simultaneously facilitates further exfoliation of the modified MoS$_2$ sheets in wet media. Although detailed analysis is beyond the scope of this work, the overall Raman spectrum characteristics for the ammonium modified MoS$_2$-based material **3a** were almost identical with that owed to **2a**, revealing that the BOC deprotection did not influence the electronic structure of MoS$_2$. Similar is the situation with the Raman spectra for the WS$_2$-based materials. In exfoliated WS$_2$, the 2LA(M), E$^1_{2g}$ and A$_{1g}$ modes were evident at 350, 355 and 419 cm^{-1}, respectively (Figure 2c). Also, other first- and second-order bands with smaller intensity were evident (e.g. 176, 230, 297, 312 and 324 cm^{-1}), however, their analysis is not relevant with the current study. The intensity of the ratio I$_{2LA(M)}$/I$_{A1g}$ was increased from 0.39 for exfoliated WS$_2$, by almost 50%, to 0.58 for **2b** and **3b**, which can be associated with the modification of WS$_2$ by the 1,2-dithiolane *tert*-butyl carbamate and the improvement of the level of exfoliation,[28] due to solubilization enhancement achieved.
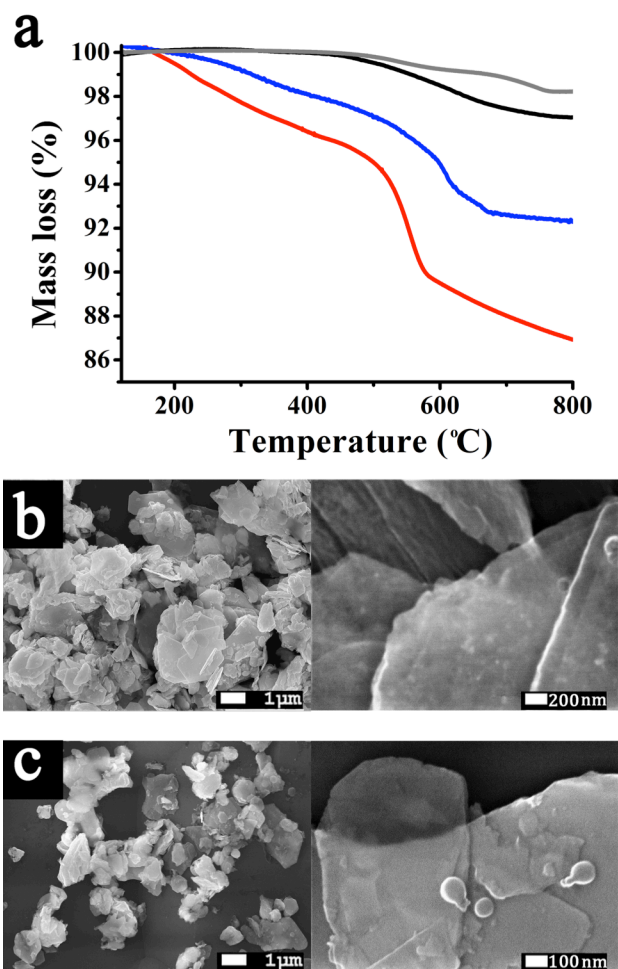

Figure 3. (a) Thermographs of ammonium modified MoS$_2$-based material **3a** (blue) and ammonium modified WS$_2$-based material **3b** (red) as compared with those of exfoliated MoS$_2$ (black) and WS$_2$ (grey), obtained under nitrogen atmosphere. (b, c) Representative FE-SEM images obtained at lower (left panel) and higher (right panel) magnification for MoS$_2$-based material **3a**, and WS$_2$-based material **3b**, respectively.

Continuing the characterization of ammonium modified **3a** and **3b** in the solid-state, thermogravimetric analysis (TGA) gave information about the stability of the materials and allowed to estimate the amount of ammonium units decorating the modified LTMDs. Under nitrogen atmosphere, **3a** and **3b** are thermally stable up to 200 ^{o}C and then starts the thermal decomposition of the organic addends that continues up to 550 ^{o}C. Beyond that temperature, decomposition of the lattice at sulfur defected sites takes place. As it is shown in Figure 3a, a mass loss of 3.2% for **3a** and 5.0% for **3b** was observed, corresponding to the loading of one organic unit per every 40 MoS$_2$ units and 41 WS$_2$ units, respectively. The relatively low loading can be safely rationalized by considering that the 1,2-dithiolane modification of MoS$_2$ and WS$_2$ network took place at the edges, where S vacancy sites were naturally introduced during the chemical exfoliation from the bulk.[21]

Morphological insight on the modified MoS$_2$ and WS$_2$ materials comes from FE-SEM imaging. Briefly, **3a** and **3b** were dispersed in MeOH and a drop was deposited onto the sample holder and
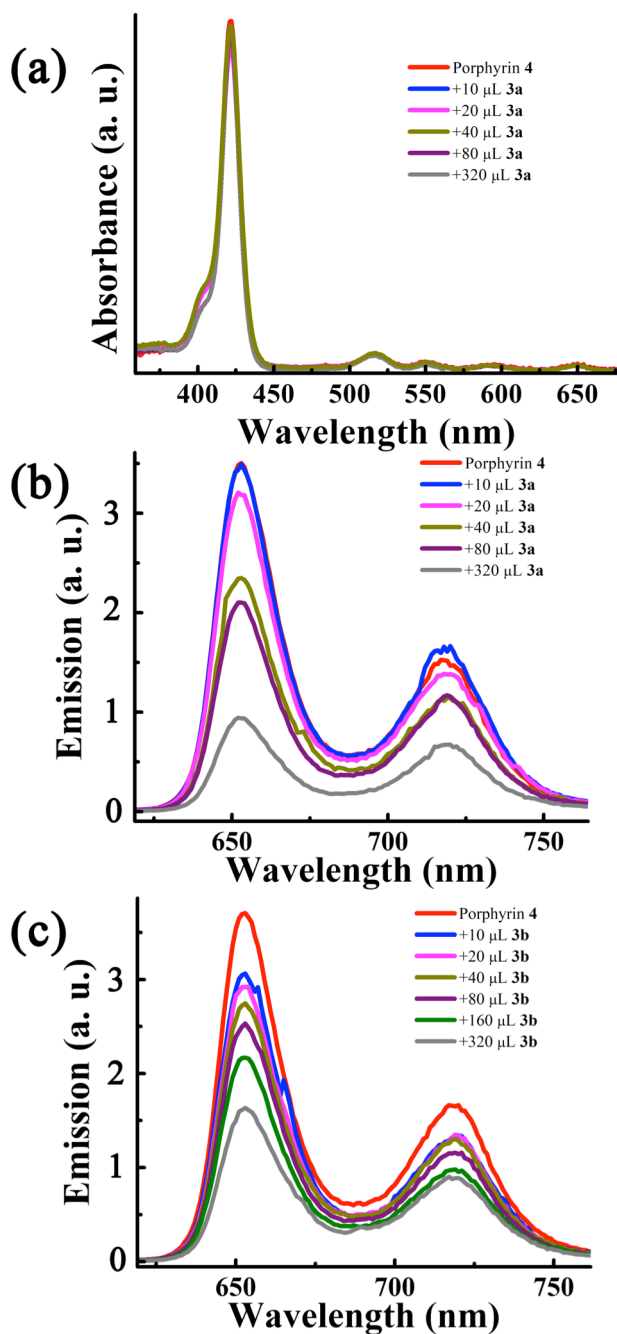
3

Figure 4. (a) Absorption spectra of anionic porphyrin **4** upon incremental additions of positively charged MoS$_2$-based material **3a**, in benzonitrile. (b, c) Emission titration assays of anionic porphyrin **4** upon incremental additions of positively charged MoS$_2$-based material **3a**, and WS$_2$-based material **3b**, respectively. Measurements were conducted in benzonitrile upon excitation at 420 nm.

thoroughly examined. Representative images for **3a** and **3b** obtained at lower and higher magnification as shown in Figure 3b, c, reveal the presence of rectangular overlapping oligolayered MoS$_2$ and WS$_2$ sheets of varied size. The observation of semi-transparent sheets can be safely associated with the presence of few (or even mono) layers of LTMDs, with lattice free of any

visible defects and absence of large bulk particles, suggesting that the functionalization methodology applied as well as the acidic treatment for the removal of the BOC protecting group did not affect the original structure of the material.

The electrostatic formation of porphyrin/MoS$_2$ **5a** and porphyrin/WS$_2$ **5b** ensembles was monitored by absorption and emission spectroscopy techniques, based on titration assays. The titration of anionic porphyrin **4** with positively charged ammonium modified materials **3a** and **3b** was performed in benzonitrile, while the concentration of the porphyrin remained invariant during the titration measurements. More precisely, a 10^{-6} M porphyrin solution was titrated by adding increasing concentrations of MoS$_2$-based material **3a** (0 to 1.3 x 10^{-5} M) or WS$_2$-based material **3b** (0 to 1.7 x 10^{-5} M) and the corresponding absorption spectra were recorded. The main features present in the UV-Vis spectrum of porphyrin **4** were at 421 nm (Soret band) and 516, 552, 592 and 650 nm (Q bands), while, any absorption spectral changes in the presence of increasing amounts of **3a** and **3b** in benzonitrile were negligible. As seen from the representative UV-Vis spectra (Figure 4a), the decrease in the intensity of the Soret band by the presence of **3a** or **3b** is not dramatic, suggesting weak electronic interactions between the two species, porphyrin and MoS$_2$ or WS$_2$, in the ground state. It should be noted that subtraction of the absorption background owed to MoS$_2$ and WS$_2$ occurred in order to allow a well-defined observation of the titration results. UV-Vis titration spectra without subtraction of the MoS$_2$ and WS$_2$ bands are presented in the Supporting Information, where the characteristic absorptions for the semiconducting phase of MoS$_2$ appear at 630 and 680 nm (Figure S2), while for WS$_2$ appear at 645 nm (Figure S3).

In stark contrast, turning to steady-state fluorescence measurements, quite strong interactions in the excited state were observed. Figure 4b shows fluorescence spectral changes of the porphyrin's emission during increased additions of positively charged ammonium modified MoS$_2$ **3a** in benzonitrile, when excited at 420 nm. Particularly, the intensity of the porphyrin-centered fluorescence, with maxima at 655 and 720 nm, was found to depend on the concentration of **3a** and progressively quenched, specifying the formation of **5a** ensembles. In an analogous fashion, quenching of the porphyrin's photoluminescence upon incremental additions of positively charged ammonium modified WS$_2$ **3b** (Figure 4c), leading to the realization of **5b** was observed. Notably, in blank titration assays of the negatively charged porphyrin **4** employing neutral **2a** and **2b** instead of the positively charged **3a** and **3b**, (Supporting Information, Figures S4 and S5, respectively), a significantly lower quenching rate for the emission of porphyrin was observed, proving the beneficial role of the electrostatic interactions between the two components for achieving effective electronic communication. Overall, these results justify the efficient deactivation of the singlet excited state of porphyrin to MoS$_2$ or WS$_2$ either via energy or electron-transfer as the effective decay mechanism.

Next, to further support the results obtained and get additional insight on the electronic interplay between porphyrin and MoS$_2$ in **5a** and WS$_2$ in **5b**, time-resolved photoluminescence studies based on the time-correlated-single-photon-counting method were performed. The fluorescence decay at 655 nm corresponding to anionic porphyrin **4** was monoexponentially fitted with a lifetime of 9.21 ns. However, by the same fitting of the fluorescence decay of **5a** and **5b**, the corresponding lifetimes were evaluated to be faster, 4.23 and 3.97 ns, respectively. The latter result is rationalized by considering appreciable Coulombic interactions between the species bearing opposite charges. Hence, transduction of energy from photoexcited porphyrin to MoS$_2$ in **5a** and WS$_2$ in **5b** occurs and

the quenching rate constant k^S_q and quantum yield Φ^S_q of the singlet excited state were calculated to be $1.43 \times 10^8\,s^{-1}$ and $1.28 \times 10^8\,s^{-1}$, and 0.57 and 0.54, for **5a** and **5b**, respectively.

In summary, we accomplished via attractive Coulombic interactions the formation of nanosized ensembles featuring modified MoS_2 and WS_2 bearing positive charges, owed to the incorporation of ammonium units, and a negatively charged porphyrin. The ensembles were fully characterized via spectroscopic (ATR-IR, Raman), thermal (TGA) and microscopy (SEM) means. Moreover, electronic absorption and photoluminescence titration assays unambiguously verified the formation of porphyrin/MoS_2 and porphyrin/WS_2 ensembles **5a** and **5b**, respectively. Finally, in combination with time-resolved photoluminescence measurements, transduction of energy from the photoexcited porphyrin, acting as electron donor, to MoS_2 or WS_2 acting as acceptors, was revealed. Overall, our findings will benefit the research community for designing and preparing advanced hybrid materials based on layered transition metal dichalcogenides and photoactive moieties useful in solar energy conversion applications.

ASSOCIATED CONTENT

Supporting Information.
Additional spectroscopic data. The Supporting Information is available free of charge on the ACS Publications website at http://pubs.acs.org.

AUTHOR INFORMATION

Corresponding Author
* Nikos Tagmatarchis, E-mail: tagmatar@eie.gr

Notes
The authors declare no competing financial interest.

REFERENCES

(1) Huang, X.; Zenga, Z.; Zhang, H. Metal Dichalcogenide Nanosheets: Preparation, Properties and Applications. *Chem. Soc. Rev.* **2013**, *42*, 1934-1946.

(2) Pumera, M.; Sofer, Z.; Ambrosi, A. Layered Transition Metal Dichalcogenides for Electrochemical Energy Generation and Storage. *J. Mater. Chem. A* **2014**, *2*, 8981-8987.

(3) Nicolosi, V.; Chhowalla, M.; Kanatzidis, M. G.; Strano, M. S.; Coleman, J. N. Liquid Exfoliation of Layered Materials. *Science* **2013**, *340*, 1226419.

(4) Miro, P.; Audiffred, M.; Heine, T. An Atlas of Two-Dimensional Materials. *Chem. Soc. Rev.* **2014**, *43*, 6537-6554.

(5) Wang, Q. H.; Kalantar-Zadeh; K., Kis, A.; Coleman J. N.; Strano, M. S. Electronics and Optoelectronics of Two-Dimensional Transition Metal Dichalcogenides. *Nature Nanotechnol.* **2012**, *7*, 699-712.

(6) Lee, K.; Gatensby, R.; McEvoy, N.; Hallam, T.; Duesberg, G. S. High-Performance Sensors Based on Molybdenum Disulfide Thin Films. *Adv. Mater.* **2013**, *25*, 6699-6702.

(7) Rowley-Neale, S.; Foster, C.; Smith, G.; Brownson D.; Banks, Mass-Producible, C. 2D-$MoSe_2$ Bulk Modified Screen-Printed Electrodes Provide Significant Electrocatalytic Performances Towards the Hydrogen Evolution Reaction. *Sustainable Energy Fuels* **2017**, *1*, 74-83.

(8) Perivoliotis, D. K.; Tagmatarchis, N. Recent Advancements in Metal-Based Hybrid Electrocatalysts Supported on Graphene and Related 2D Materials for the Oxygen Reduction Reaction. Carbon **2017**, *118*, 493-510.

(9) Stephenson, T.; Li; Z.; Olsen, B.; Mitlin, D. Lithium Ion Battery Applications of Molybdenum Disulfide (MoS_2) Nanocomposites. *Energy Environ. Sci.* **2014**, *7*, 209-231.

(10) Xu, M.; Liang, T.; Shi, M.; Chen, H. Graphene-Like Two-Dimensional Materials. *Chem. Rev.* **2013**, *113*, 3766-3798.

(11) Niu, L.; Coleman, J.; Zhang, H.; Shin, H.; Chhowalla, M.; Zheng, Z. Production of Two-Dimensional Nanomaterials via Liquid-Based Direct Exfoliation *Small* **2015**, *12*, 272-293.

(12) Pagona, G.; Bittencourt, C.; Arenal R.; Tagmatarchis, N. Exfoliated Semiconducting Pure 2H-MoS_2 and 2H-WS_2 Assisted by Chlorosulfonic Acid. *Chem. Commun.* **2015**, *51*, 12950-12953.

(13) Zheng, J.; Zhang, H.; Dong, S.; Liu, Y.; Nai, C. T.; Shin, H. S.; Jeong, H. Y.; Liu, B.; Loh, K. P. High Yield Exfoliation of Two-Dmensional Chalcogenides using Sodium Naphthalenide. *Nature Commun.* **2014**, *5*, 2995-2999.

(14) Yao, Y.; Tolentino, L.; Yang, Z.; Song, X.; Zhang, W.; Chen, Y.; Wong, C.-P. High Concentration Aqueous Dispersions of MoS_2. *Adv. Funct. Mater.* **2013**, *23*, 3577-3583.

(15) Lee, C.; Li, Q. Y.; Kalb, W.; Liu, X. Z.; Berger, H. R.; Carpick, W.; Hone, J. Frictional Characteristics of Atomically Thin Sheets. *Science* **2010**, *328*, 76-80.

(16) Matte, H. S. H. R., Gomathi, A.; Manna, A. K.; Late, D. J.; Datta, R.; Pati S. K.; Rao, C. A. N. R. MoS_2 and WS_2 Analogues of Graphene. *Angew. Chem. Int. Ed.* **2010**, *49*, 4059-4062.

(17) Zeng, Z.; Yin, Z.; Huang, X.; Li, H.; He, Q.; Lu, G.; Boey F.; Zhang, H. Single-layer Semiconducting Nanosheets: High-Yield Preparation and Device Fabrication. *Angew. Chem. Int. Ed.* **2011**, *50*, 11093-11097.

(18) Chen, X.; McDonald, A. R. Functionalization of Two Dimensional Transition Metal Dichalcogenides. *Adv. Mater.* **2016**, *28*, 5738-5746.

(19) Voiry, D.; Goswami, A.; Kappera, R.; C. C. Silva, Kaplan, D.; Fujita, T.; Chen, M.; Asefa, T.; Chhowalla, M. Covalent Functionalization of Monolayered Transition Metal Dichalcogenides by Phase Engineering. *Nature Chem.* **2015**, *7*, 45-49.

(20) Knirsch, K. C.; Berner, N. C.; Nerl, H. C.; Cucinotta, C. S.; Gholamvand, Z.; McEvoy, N; Wang, Z.; Abramovic, Vecera, I. P.; Halik, M.; Sanvito, S.; Duesberg, G. S.; Nicolosi, V.; Hauke, F.; Hirsch, A., Coleman J. N.; Ba-

ckes, C. Basal-Plane Functionalization of Chemically Exfoliated Molybdenum Disulfide by Diazonium Salts. *ACS Nano,* **2015**, *9*, 6018-6030.

(21) Canton-Vitoria, R.; Sayed-Ahmad-Baraza, Y.; Pelaez-Fernandez, M.; Arenal, R.; Bittencourt, C.; Ewels C. P.; Tagmatarchis, N.; Functionalization of MoS_2 with 1, 2-dithiolanes: Toward Donor-Acceptor Nanohybrids for Energy Conversion. *NPJ 2D Mater. Appl.* **2017**, *1*, 13.

(22) Torre, G. D.; Bottari, G.; Sekita, M. Hausmann, A.; Guldi, D. M.; Torres T. A Voyage into the Synthesis and Photophysics of Homo- and Heterobinuclear Ensembles of Phthalocyanines and Porphyrins. *Chem. Soc. Rev.* **2013**, *42*, 8049-8105.

(23) Souza, F. D.; Kadish, K. M. *Handbook of Carbon Nano Materials*: *Synthesis and supramolecular systems*; World Scientific: Singapore*, 2011.

(24) Bottari, G.; Herranz, M. A.; Wibmer, L.; Volland, M.; Rodrıguez-Perez, L.; Guldi, D. M.; Hirsch, A.; Martın, N.; Souza F. D.; Torres, T. Chemical Functionalization and Characterization of Graphene-Based Materials. *Chem. Soc. Rev.* **2017**, *46*, 4464-4500.

(25) Bottari, G.; Trukhina, O.; Ince, M.; Torres, T. Towards Artificial Photosynthesis: Supramolecular, Donor–Acceptor, Porphyrin- and Phthalocyanine/Carbon Nanostructure Ensembles. *Coord. Chem. Rev.* **2012**, *256*, 2453-2477.

(26) Zhang, N.; Yang, M. Q.; Liu, S.; Sun, Y.; Xu, Y.J. Waltzing with the Versatile Platform of Graphene to Synthesize Composite Photocatalysts. *Chem. Rev.* **2015**, *115*, 10307-10377.

(27) Pimenta, M. A.; del Corro, E.; Carvalho, B. R.; Fantini, C.; Malard, L. M. Comparative Study of Raman Spectrscopy in Graphene and MoS_2-type Transition Metal Dichalcogenides. *Acc. Chem. Res*. **2015**, *48*, 41-47.

(28) Berkdemir, A.; Gutiérrez, H. R.; Botello-Méndez, A. R.; Perea-López, N.; Elías, A. L.; Chia, C. I.; Terrones, H. Identification of Individual and Few Layers of WS_2 Using Raman Spectroscopy. *Sci. Rep.* **2013**, *3*, 1755.